Heliyon 8 (2022) e10965

Contents lists available at ScienceDirect

Heliyon

journal homepage: www.cell.com/heliyon

Research article

Differential plasma proteomes of the patients with *Opisthorchiasis viverrini* and cholangiocarcinoma identify a polymeric immunoglobulin receptor as a potential biomarker

Sattrachai Prasopdee [a,b], Yodying Yingchutrakul [c], Sucheewin Krobthong [d,e], Montinee Pholhelm [a,b], Patompon Wongtrakoongate [d,f], Kritiya Butthongkomvong [g], Jutharat Kulsantiwong [h], Teva Phanaksri [b], Anthicha Kunjantarachot [b], Thanakrit Sathavornmanee [i], Smarn Tesana [a], Veerachai Thitapakorn [a,b,*]

[a] *Thammasat Research Unit in Opisthorchiasis, Cholangiocarcinoma, and Neglected Parasitic Diseases, Thammasat University, Pathum Thani 12120, Thailand*
[b] *Chulabhorn International College of Medicine, Thammasat University, Pathum Thani 12120, Thailand*
[c] *Proteomics Research Team, National Omics Center, NSTDA, Pathum Thani 12120, Thailand*
[d] *Center for Neuroscience, Faculty of Science, Mahidol University, Bangkok 10400, Thailand*
[e] *Interdisciplinary Graduate Program in Genetic Engineering, Kasetsart University, Bangkok 10900, Thailand*
[f] *Department of Biochemistry, Faculty of Science, Mahidol University, 10400 Bangkok, Thailand*
[g] *Medical Oncology Unit, Udonthani Cancer Hospital, Ministry of Public Health, Udon Thani 41330, Thailand*
[h] *Faculty of Science, Udon Thani Rajabhat University, Udon Thani 41000, Thailand*
[i] *Chonburi Hospital, Ministry of Public Health, Chonburi 20000, Thailand*

ARTICLE INFO

Keywords:
Plasma proteome
LC-MS/MS
Cholangiocarcinoma
Opisthorchis viverrini
S100A9
PIGR

ABSTRACT

In Southeast Asian countries, nitrosamine compounds and the liver fluke *Opisthorchis viverrini* have long been identified as carcinogens for cholangiocarcinoma (CHCA). In order to effectively treat *O. viverrini* infections and prevent the development of CHCA, methods for disease detection are needed. This study aims to identify biomarkers for *O. viverrini* infection and CHCA. In the discovery phase, technical triplicates of five pooled plasma pools (10 plasma each) of healthy control subjects (noOVCCA), *O. viverrini* subjects (OV), and cholangiocarcinoma subjects (CCA), underwent solution-based digestion, with the label-free method, using a Thermo Scientific™ Q Exactive™ HF hybrid quadrupole-Orbitrap mass spectrometer and UltiMate 300 LC systems. The noOVCCA, OV, and CCA groups demonstrated different profiles and were clustered, as illustrated by PCA and heat map analysis. The STRING and reactome analysis showed that both OV and CCA groups up-regulated proteins targeting immune system-related proteins. Differential proteomic profiles, S100A9, and polymeric immunoglobulin receptor (PIGR) were specifically expressed in the CCA group. During the validation phase, another 50 plasma samples were validated via the PIGR sandwich ELISA. Using PIGR >1.559 ng/ml as a cut-off point, 78.00% sensitivity, 71.00% specificity, and AUC = 0.8216, were obtained. It is sufficient to differentially diagnose cholangiocarcinoma patients from healthy patients and those with *Opisthorchiasis viverrini*. Hence, in this study, PIGR was identified and validated as a potential biomarker for CHCA. Plasma PIGR is suggested for screening CHCA, especially in an endemic region of *O. viverrini* infection.

1. Significance of the study

By differentiating the proteomic profiles of healthy control subjects, *Opisthorchiasis viverrini* subjects, and cholangiocarcinoma subjects, the S100A9 and polymeric immunoglobulin receptor (PIGR) were identified as potential biomarkers for cholangiocarcinoma. The plasma PIGR concentration was further validated for its potential as a diagnostic biomarker. The results demonstrate that the plasma PIGR concentration was significantly higher in cholangiocarcinoma subjects than in patients only infected with *O. viverrini*, as well as control subjects ($P < 0.05$). The sensitivity, specificity, and accuracy were obtained. This suggests plasma PIGR is a potential biomarker for

* Corresponding author.
E-mail address: veebkk@gmail.com (V. Thitapakorn).

https://doi.org/10.1016/j.heliyon.2022.e10965
Received 22 April 2022; Received in revised form 10 August 2022; Accepted 30 September 2022

screening cholangiocarcinoma, especially in an endemic area of *O. viverrini*.

2. Introduction

Cholangiocarcinoma (CHCA), a bile duct cancer, is a nefarious disease due to its initial asymptomatic nature, resulting in a high mortality rate (Banales et al., 2020). Globally, CHCA is an uncommon disease; high prevalence and incidence rates have been reported in Southeast Asian countries, including Thailand, owing to the endemic liver fluke *Opisthorchis viverrini* (Steele et al., 2018). Infections due to *O. viverrini* and its sister taxa *O. felineus*, as well as *Clonorchis sinensis*, have been verified as carcinogens for CHCA (IARC, 1994). In non-endemic areas, however, primary sclerosing cholangitis (PSC), chronic inflammation, is a premalignant condition that leads to CHCA (Banales et al., 2020). *O. viverrini* infections are present in raw or undercooked fishes containing the parasite's metacercariae. Chronic infections with *O. viverrini* result in DNA damage due to reactive oxygen species, inflammation, accumulated mutations, and, ultimately, CHCA (Pinlaor et al., 2003, 2009; Prakobwong et al., 2011). To prevent CHCA, it is vital that *O. viverrini* infections be diagnosed early and treated with the antihelminthic drug praziquantel. Furthermore, the early detection of CHCA in its asymptomatic stages allows for better chemotherapeutic response and overall survival. Detecting host-responsive proteins may help detect *O. viverrini* infections and/or early-stage CHCA. To identify specific proteins for use as biomarkers, the proteomics-based LC-MS/MS approach was applied. In this study, differential plasma proteomic profiles of non-*O. viverrini* infection and non-cholangiocarcinoma subjects (noOVCCA), *O. viverrini* subjects (OV), and cholangiocarcinoma subjects (CCA) were investigated. The Thermo Scientific™ Q Exactive™ HF hybrid quadrupole-Orbitrap mass spectrometer was used to identify the potential biomarkers for *O. viverrini* infections and CHCA.

3. Materials and methods

3.1. Chemicals and reagents

Trypsin was obtained from Promega (Promega Co., Madison, WI, USA). UV-Vis spectroscopy was performed using the Synergy H1 microplate reader (BioTek Corp., HT, USA). Sodium dodecyl sulfate (SDS), acetonitrile (analytical grade), acetic acid (glacial), acetone (AR), HEPES sodium salt hydrate, potassium hydroxide (KOH), ammonium bicarbonate, Tris HCl, and formic acid (LC-MS grade) were all obtained from Sigma-Aldrich. An iodoacetamide (IAA) and dithiothreitol (DTT) were purchased from GE Healthcare. RapidGest SF Surfactant was obtained from Waters. The acetonitrile (ultra-LC-MS) and LC-MS-grade water were purchased from J.T. Baker (Thermo Fisher Scientific, Loughborough, UK).

3.2. Subjects

The protocol of this study was approved by the Human Ethics Committee of Udonthani Cancer Hospital, Udon Thani, Ministry of Public Health, Thailand, protocol number UCH-CT 11/2563. The fecal examination for *O. viverrini* eggs, liver ultrasonography, and histopathology were used to classify subjects. During the discovery phase, 50 subjects of each group were analyzed using LC-MS/MS-based proteomics. During the validation phase, another 50 subjects in each group were analyzed using the sandwich ELISA method. The subjects were divided into three groups based on their health statuses. Subjects with a normal physical examination, no liver enlargement or jaundice, and negative for *O. viverrini* eggs on fecal examination were assigned to the healthy control group (noOVCCA). Subjects positive for *O. viverrini* eggs on fecal examination with normal liver by ultrasonography were recruited to the *O. viverrini*-infected group (OV). Subjects with hepatomegaly and/or jaundice on physical examination, abnormal liver ultrasonography, and CHCA confirmed on liver tissue histopathology were assigned to the cholangiocarcinoma group (CCA). Subjects in the noOVCCA and CCA groups were recruited from Udonthani Cancer Hospital, Udon Thani, Thailand. Subjects in the OV group were recruited during the annual health check-ups at health promotion hospitals in Nong Khai province, Thailand. All subjects in the OV group were asymptomatic with low intensity of infection or light infection (<1000 EPG) (Boondit et al., 2020; Maleewong et al., 1992). Recruitment criteria, group allocation, and a summary of the clinical statuses of subjects are summarized in Figure 1 and Table 1.

3.3. Blood collection and plasma preparation

Blood was collected from the median cubital vein using a 21 G needle. EDTA was used as an anti-coagulant. Plasma was collected by mixing by inverting the blood before spinning at 3000x *g* for 10 min at room temperature. The plasma was then collected and aliquoted to avoid freeze–thaw cycles and kept at −80 °C until used.

3.4. Sample preparation for gel-free-based proteomes

A triplicate of 5 pooled plasma pools (10 plasma each) of each group (technical triplicate of 5 biological replicates) was used in this study (Supplementary File 1). Protein concentrations of plasma were measured using Lowry's method (*DC* Protein Assay, Bio-Rad, USA) with bovine serum albumin as the standard reference (2–10 μg/μL). The pooled plasma was prepared by pooling equal amounts of protein from each subject (100 μg each). For each group, the 5 pooled plasma samples were prepared by pooling 10 individual plasma samples each. Finally, 5 pooled plasma samples/group of all 3 groups were prepared (15 pooled plasma samples in total). The plasma proteins were prepared and analyzed as previously described (Krobthong et al., 2021) with minor modifications. Briefly, 50 μL of pooled plasma proteins were mixed with 50 μL of fresh lysis buffer solution (0.2% SDS, 20 mM DTT, in 10 mM HEPES-KOH, pH 8.0). The protein solution was precipitated by using 500 μL of cold acetone at −20 °C for 24 h. The protein pellet was collected and reconstituted in 0.2% RapidGest SF (Waters Co., UK) in 10 mM ammonium bicarbonate. The protein concentration was re-measured, and 25 μg of protein was then subjected to trypsin digestion with the following protocol with minor modifications. Briefly, 5 mM DTT was used to reduce proteins by incubating at 60 °C for 20 min. Alkylation of the reduced proteins was conducted using 20 mM IAA for 30 min at room temperature in the dark. The alkylated proteins were cleaned up to remove the remaining DTT and IAA by a 7 kDa molecular weight cut-off (Zeba™ Spin Desalting Columns, Thermo Fisher Scientific, USA). Proteolytic digestion was performed using 500 ng of trypsin (Promega, Germany) and incubated at 37 °C for 3 h. The tryptic peptides were dried, resolubilized in 0.1 % formic acid, and objected to a TruView LC-MS vial (Waters).

3.5. LC-MS/MS setting for protein identification and quantification

Proteomics data analysis was conducted in data-dependent mode using LC-MS/MS, Thermo Scientific™ Q Exactive™ HF hybrid quadrupole-Orbitrap mass spectrometer, and an UltiMate 3000 LC system. The tryptic peptides were analyzed by LC-MS/MS with minor modification (Krobthong et al., 2022). Briefly, the tryptic peptides were desalted (C18 PepMap-100 trapping column) and resolved by C18 PepMap™ capillary column (25 cm long) with a 70 min long gradient of acetonitrile and 0.1% formic acid at a flow rate of 0.3 μL/min. The MS spectra were acquired under the following conditions: m/z 400–1600, AGC target set at 3×10^6 ions, and a 60 k resolution. MS2 scan was initiated when the ACG target set reached 1×10^5 ions. An ion selection was completed within 12 s of the dynamic exclusion window. Proteome Discoverer software version 2.4 (Thermo Fisher Scientific), including SEQUEST, Percolator, and Minora algorithms, were used to analyze the raw spectrum files. The peptide was compared with the Human UniProtKB database (20,394 sequences on 12/02/2020). The following

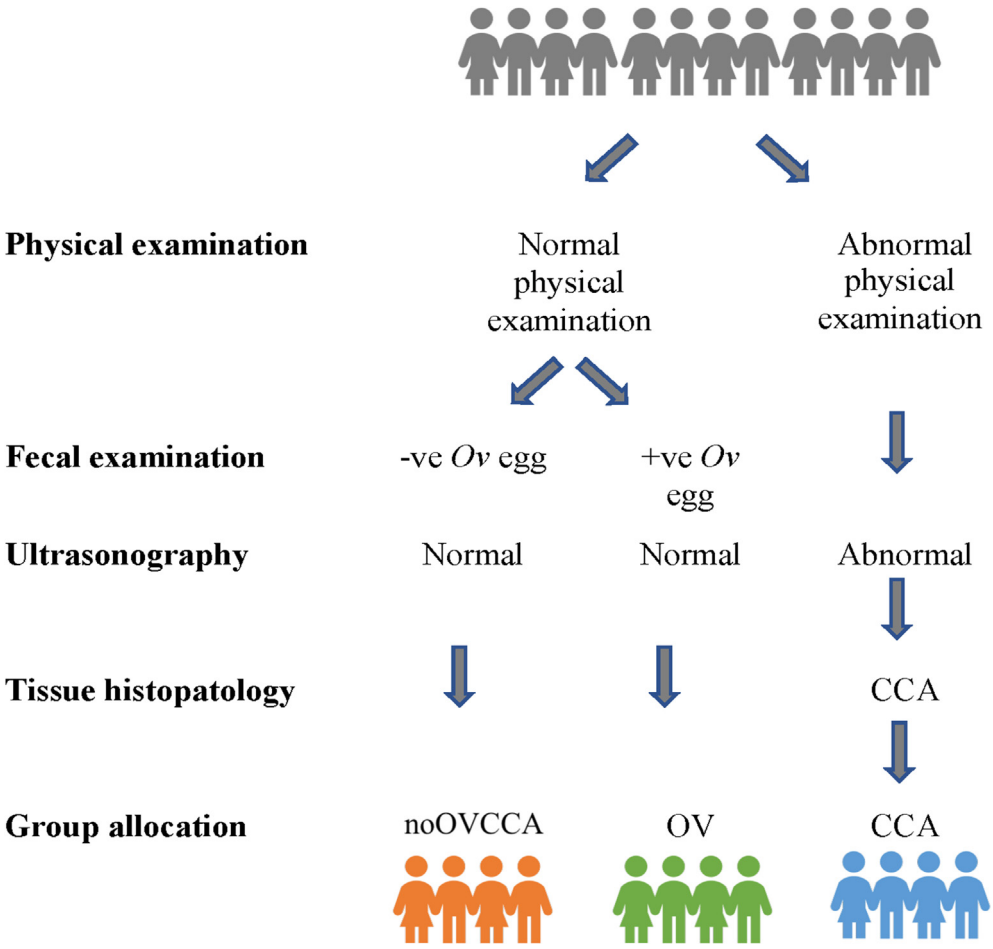

Figure 1. Recruitment of participants. The physical examination, stool examination of *O. viverrini* egg, liver ultrasonography, and tissue histopathology were used for group allocation.

parameters were used for protein identification and quantification: two trypsin missed cleavages as maximum, 10 ppm of precursor mass tolerance, 0.1 Da of fragment mass tolerance, carbamidomethylation (cysteine, static modifications), and oxidation (methionine, dynamic modifications). The false discovery rate (FDR) of 0.01 was selected and used for peptide and protein identification. Total peptide amount was used for normalizing relative protein abundance ratios. All proteome data were submitted to the ProteomeXchange Consortium via the PRIDE partner repository (Vizcaino et al., 2013). Dataset identifier: PXD028152; Project Name: Serum proteomics analysis of CCA; Project accession: PXD028152; Project DOI: 10.6019/PXD028152; Username: reviewer_pxd028152@ebi.ac.uk; and Password: IHy85xct.

3.6. Bioinformatics and identification of potential biomarkers

To investigate the heterogeneity of plasma variation in noOVCCA, OV, and CCA subjects, principal component analysis (PCA) was used to observe the differences by Proteome Discoverer. Three-dimensional PCA was conducted by Plotly (R Studio). The heatmap was constructed using the Proteome Discoverer software for hierarchical clustering. Jvenn was used to plot the Venn diagram (Bardou et al., 2014). The specific proteins of each proteome were then used for predicting protein–protein interactions by STRING (Szklarczyk et al., 2021). Reactomes were used to analyze biological networks based on the Reactome Pathway Database (http://www.reactome.org). The significant threshold for altered biological pathways was set at a $P < 0.01$ (Haw et al., 2011). The proteins found in the CCA group by the Venn diagram were found in all 15 replicates of the CCA group and were selected and identified as potential biomarkers.

3.7. Measurement of plasma PIGR by sandwich enzyme-linked immunosorbent assay

Validation of identified proteins for CHCA was performed on plasma PIGR using the sandwich ELISA method (Human PIGR ELISA Pair Set, Sino Biological Inc., Beijing, China) following the company-provided protocol. Plate washing of the following step was conducted using 300 μl of washing buffer (20 mM Tris, 150 mM NaCl, pH 7.4, and 0.05% Tween®20) (microplate washer, APW-100, Allsheng) 3 times each. Another 50 plasma samples in each subject group were used to verify the potential as a diagnostic biomarker for CHCA using plasma PIGR. For each sample, plasma diluted to 1:50 was used and performed in duplicates. The standard human PIGR of 0–312.5 ng/ml was prepared and used for a standard curve plot. The capture antibody was diluted by coating buffer pH 9.6 (0.05 M Na_2CO_3, 0.05 M $NaHCO_3$, and filter sterile) to 2 μg/ml, and 100 μl of diluted capture antibody was then added to a 96-well ELISA plate (Maxisorp, NUNC) and incubated at 4 °C overnight. The plates were washed, blocked for non-specific binding using 300 μl of blocking buffer (2% bovine serum albumin in washing buffer), and incubated for 1 h at room temperature. The plates were washed, and each 100 μl of the diluted plasma samples and standards in sample dilution buffer (0.1% BSA in washing buffer) were added and incubated at room temperature for 2 h. The plates were washed, and 100 μl of 1 μg/ml detection antibody diluted in detection antibody dilution buffer (0.5% BSA in washing buffer) was then added and incubated for 1 h at room temperature. The plates were washed, 200 μl of TMB substrate solution (0.1 mg/ml 3,3,5,5-tetramethylbenzidine [Sigma] diluted in 10 ml of 0.05 M citrate

Table 1. The demographic and clinical statuses of subjects. The alcohol consumption, smoking, raw fish eating-habit, and history of *O. viverrini* infection were highest in CCA subjects when compared to noOVCCA and OV subjects.

	Discovery phase by LC-MS/MS			Validation phase by ELISA		
	noOVCCA	OV	CCA	noOVCCA	OV	CCA
Sample size	50	50	50	50	50	50
Sex (Male/Female)	16/34	28/22	38/12	21/29	29/21	29/21
Age (year)						
Min/Max	20/59	33/75	45/84	21/60	18/79	32/87
Mean ± SD	38.36 ± 9.45	55.56 ± 9.10	61.12 ± 7.70	38.44 ± 9.99	54.08 ± 13.64	60.12 ± 10.66
Alcohol consumption						
No	33 (66%)	26 (52%)	10 (20%)	20 (40%)	14 (28%)	15 (30%)
Yes	17 (34%)	24 (48%)	40 (80%)	30 (60%)	36 (72%)	35 (70%)
Smoking						
No	42 (84%)	32 (64 %)	18 (36%)	38 (76%)	28 (56%)	24 (48%)
Yes	8 (16%)	18 (36 %)	32 (64%)	12 (24%)	22 (44%)	26 (52%)
Raw fish eating-habit (Source of *O. viverrini* infection)						
No	33 (66%)	10 (20%)	8 (16%)	33 (66%)	5 (10%)	7 (14%)
Yes	17 (34%)	40 (80%)	42 (84%)	16 (32%)	45 (90%)	42 (84%)
Uncertain	0 (0%)		0 (0%)	1 (2%)		1 (2%)
History of *O. viverrini* infection						
No	50 (100%)	42 (84%)	36 (68%)	48 (96%)	45 (90%)	37 (76%)
Yes	0 (0%)	8 (16%)	11 (22%)	1 (2%)	5 (10%)	12 (24%)
Uncertain	0 (0%)	0 (0%)	3 (6%)	1 (2%)	0 (0%)	1 (2%)
Fermented food eating-habit (Source of nitrosamine)						
No	2 (4%)	0 (0%)	0 (0%)	3 (6%)	0 (0%)	0 (0%)
Yes	48 (96%)	50 (100%)	50 (100%)	47 (94%)	50 (100%)	49 (98%)
Uncertain	0 (0%)	0 (0%)	0 (0%)	0 (0%)	0 (0%)	1 (2%)
Cancer stage						
Stage 1 (%)	0 (0%)	0 (0%)	1 (2%)	0 (0%)	0 (0%)	1 (2%)
Stage 2 (%)	0 (0%)	0 (0%)	5 (10%)	0 (0%)	0 (0%)	0 (0%)
Stage 3 (%)	0 (0%)	0 (0%)	1 (2%)	0 (0%)	0 (0%)	1 (2%)
Stage 4 (%)	0 (0%)	0 (0%)	43 (86%)	0 (0%)	0 (0%)	48 (96%)

phosphate buffer pH 5.0, and 2 μl of 30% H_2O_2) was added, and they were incubated in the dark at room temperature for 20 min. To stop the reaction, 2 N H_2SO_4 was added, and the absorbance values were measured at 450 nm. The absorbance of each sample and standards were subtracted with zero standard absorbance. The log (PIGR standard concentration, ng/ml) values were plotted against subtracted OD450 and used as a standard curve for PIGR concentration calculation. PIGR concentrations (ng/ml) were then calculated using the linear equation shown in the graph below.

3.8. Statistical and diagnostic analyses

The IBM SPSS Statistics for Windows, version 26.0 (IBM Corp, Armonk, NY, USA) was used. Statistically significant differences between the PIGR concentration of each group were determined by one-way analysis of variance (ANOVA) followed by a subsequent Scheffe post-hoc test. GraphPad Prism 9 was used for analyzing the dot plot and the area under the receiver operating characteristic curve (AUC). Diagnostic parameters were calculated using the diagnostic test evaluation calculator (MedCalc Software, available at https://www.medcalc.org/calc/diagnostic_test.php), including the sensitivity, specificity, positive predictive value (PPV), negative predictive value (NPV), and accuracy.

4. Results

4.1. Analysis of plasma proteomes

The proteomics data was submitted to the ProteomeXchange Consortium via the PRIDE partner repository with the dataset identifier PXD028152 (Vizcaino et al., 2013). PCA and heatmap analyses of the triplicate of 5 pooled plasma pools of each group of noOVCCA, OV, and CCA showed differences in proteome profiles. The PCA results (Figure 2A, 2B, and 2C) were consistent with the heatmap (Figure 2D); within-group protein differences were smaller than between-group differences. By plotting PC1 against PC2 and PC1 against PC3, noOVCCA (orange circle) was more closely related to OV (green circle) than CCA (blue circle) (Figure 2A, 2B, and 2C), similar to the results found in the heatmap (Figure 2D). Differences in expressed plasma proteins among each group were clustered hierarchically, as presented in Figure 2D. The heatmap depicts their relative abundance with color coding (down- and up-regulated levels: green to red, respectively). The patterns of down- and up-regulation of protein profiles in CCA differed from the noOVCCA and OV groups. The green vertical line remarks the node of CCA down-regulated proteins, and red vertical line remarks the node of CCA up-regulated proteins (Figure 2D).

4.2. Differential proteome profiles

To investigate the pathogenesis-related proteins of *O. viverrini* infections and cholangio-carcinogenesis, differential plasma proteomes, including noOVCCA vs. OV, noOVCCA vs. CCA, and OV vs. CCA, were analyzed further by jvenn (Venn diagram), STRING, and reactome analysis. STRING and reactome analysis results were in agreement. The STRING results of CCA-specific proteins were targeted to the immune system, coagulation factors, and motor-related proteins (Figure 3), while OV-specific proteins were targeted to the motor and chromosome-related proteins and coagulation factors (Figure 3). Interestingly, the OV and CCA shared proteins were targeted to cell adhesion and activation of T cells (Figure 3). For reactome analysis, specific proteins of both OV and CCA groups

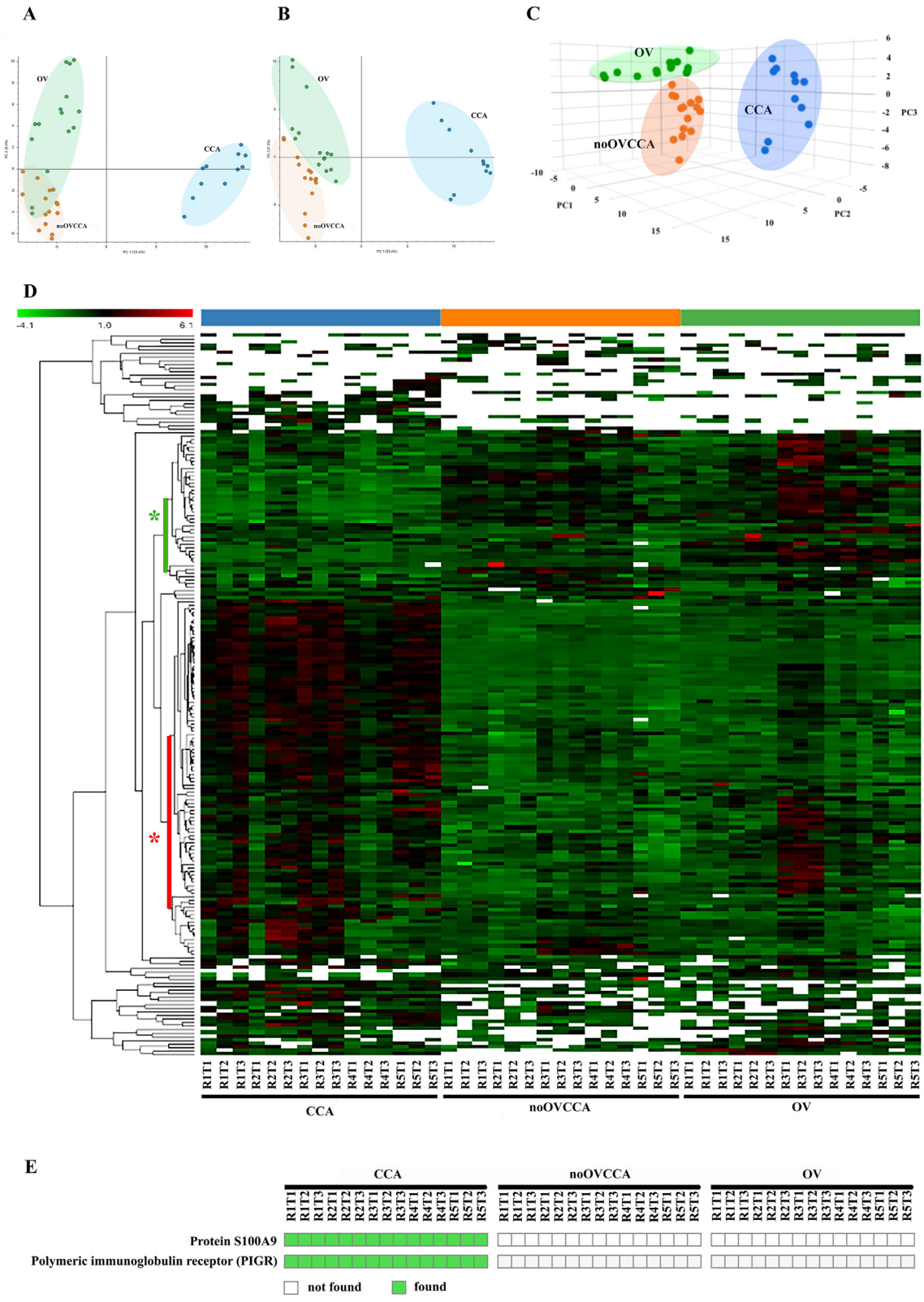

Figure 2. Principal component analysis (PCA) and heat map of noOVCCA, OV, and CCA groups. The orange, green, and blue colors represent noOVCCA, OV, and CCA groups, respectively. (A) PC1 to PC2 and (B) PC1 to PC3. (C) Three-dimensional plot of PCA. (D) Heat map of noOVCCA, OV, and CCA groups. The green to red color bar indicates the peak intensity from low to high, respectively. The R and T indicate biological replicate (R1-5) and technical replicate (T1-3), respectively. The green vertical line remarks the node of CCA down-regulated proteins, and the red vertical line remarks the node of CCA up-regulated proteins. (E) Identification of potential biomarkers by differential proteomes. The protein S100A9 and polymeric immunoglobulin receptor (PIGR) are identified as potential biomarkers for CCA. The green color box indicates the peptide peak is matched and found in each replicate and the white color box indicates peptide is not found. PCA and heat map clearly discriminated CCA from noOVCCA and OV.

belonged to the hierarchy of the immune system, homeostasis, signal transduction, and metabolism (Supplementary Files 2 and 3). For the comparison of OV to healthy controls, the immune system hierarchy (MHC class I, interferon, antigen processing, and presentation), metabolism (fat-soluble vitamins, especially vitamin A), and disease are shown (Supplementary File 2). Comparisons between CCA and healthy controls revealed specific pathways of the immune system (TLR, cytokine, antigen processing, and presentation), signal transduction (Rho GTPases and JAK/STAT), and disease (TLR signaling cascade of the immune system). The significant pathways are shown in Supplementary File 3. Overall, results suggested that OV- and CCA-specific proteins were targeted to the immune system and immune system-related signaling pathways.

4.3. Identification of potential biomarkers

In this study, the "present" and "absent" criteria were used to identify potential biomarkers for *O. viverrini* infection and cholangiocarcinoma. Unfortunately, no proteins specific to *O. viverrini* infection were identified in this study. However, polymeric immunoglobulin receptor (PIGR) and S100A9 were explicitly found in the CCA group proteome with potential as a cholangiocarcinoma biomarker (Figure 2E). S100A9 has been identified

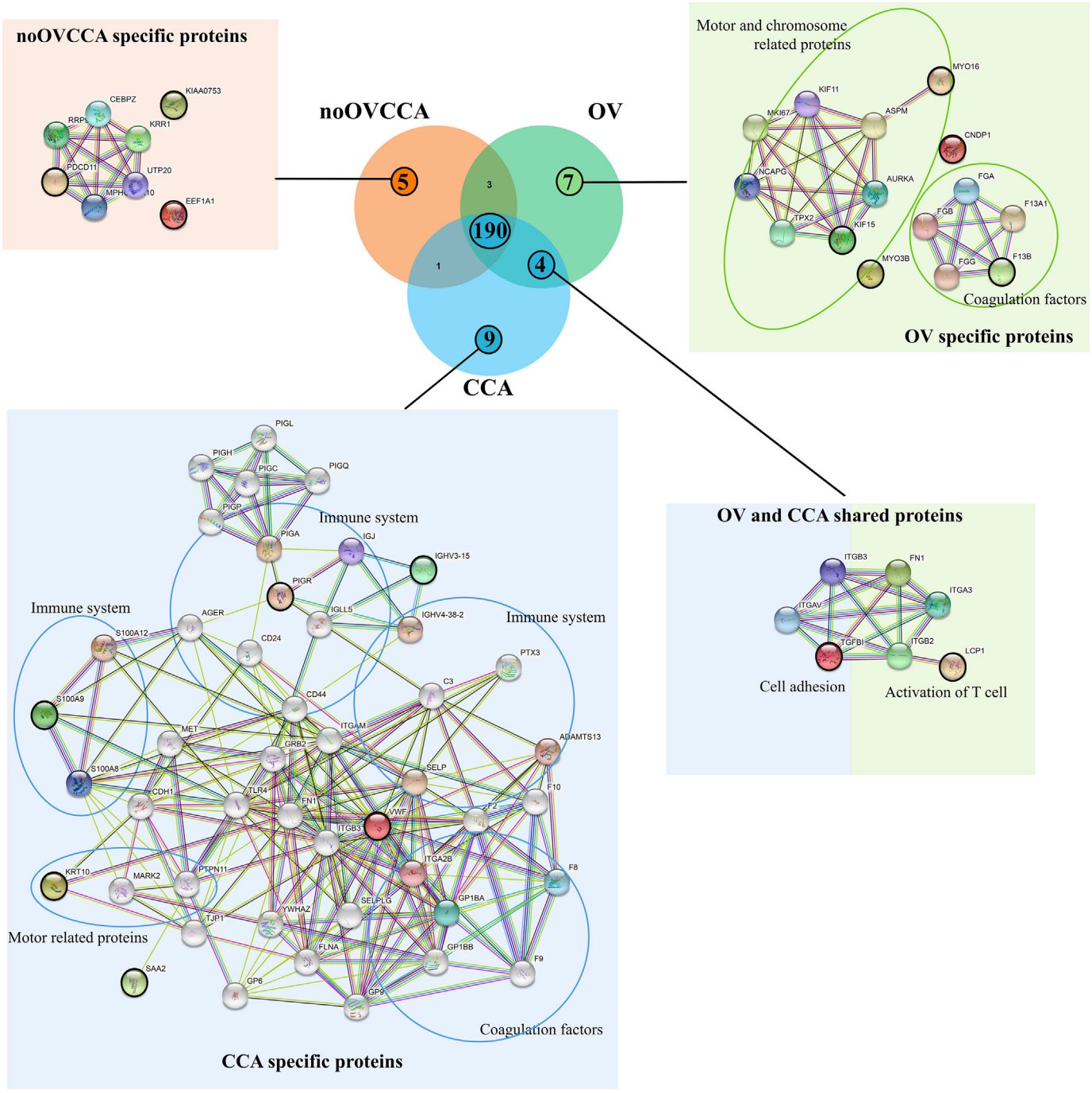

Figure 3. Protein-protein interaction of noOVCCA, OV, and CCA-specific proteins by STRING. The motor and chromosome-related proteins and coagulation factors were linked to OV while the immune system-related proteins were additionally linked to the CCA protein network.

and validated as a potential biomarker for CHCA (Duangkumpha et al., 2019). Therefore, the PIGR was focused on in this study. From LC-MS/MS results, five peptides of PIGR were specifically identified in all CCA proteome replicates, including 123-YLCGAHSDGQLQEGSPIQAWQLFV-NEESTIPR-154, 193-LDIQGTGQLLFSVVINQLR-211, 232-NADLQVLKPE-PELVYEDLRGSVTFHCALGPEVANVAK-268, 297-ILLNPQDKDGSFSVVIT GLR-316, 526-LVSLTLNLVTR-536. These five peptides exclusively belonged to the CCA proteome; therefore, PIGR was identified as a potential biomarker for CHCA and further validated by sandwich ELISA.

4.4. Validation of plasma PIGR concentration as a potential biomarker

Plasma PIGR concentration based on sandwich ELISA was calculated from a linear equation ($R^2 = 0.9789$) of PIGR to a standard log (concentration) curve against an OD of 450 nm. The result showed that the concentrations of plasma PIGR were lowest in the OV group and highest in the CCA group (Figure 4). The average concentrations (ng/ml) ± SD of plasma PIGRs of noOVCCA, OV, and CCA were 1.4936 ± 0.6085, 1.3309 ± 0.5248, and 6.0942 ± 7.5840, respectively (Supplementary File 4). One-way ANOVA revealed that at least two groups had significantly different concentrations of PIGR ($P < 0.01$). The Scheffe test for multiple comparisons further revealed that the mean plasma PIGR concentration of the CCA group was significantly different from the OV group ($P < 0.01$; 95% CI: 2.585, 6.941) and the noOVCCA group ($P < 0.01$; 95% CI: 2.422, 6.778). However, there were no significant differences between the OV group and the noOVCCA group ($P = 0.98$; 95% CI: −2.340, 2.014). The AUC of noOVCCA and OV vs. CCA was 0.8216 (Figure 5). The highest AUC (0.8778) was obtained from OV vs. CCA (Figure 5). Using >1.559 ng/ml PIGR cut-off, 78.00% sensitivity, 71.00% specificity, 57.35% positive predictive value, 86.59% negative predictive value, and 73.33% accuracy were obtained (Table 2). However, using plasma PIGR >3.850 as a cut-off, the 100% specificity of the test was obtained with limited sensitivity (Table 2). Hence, the LC-MS/MS, Venn diagram, and ELISA results were consistent and indicated that PIGR was highly specific to CHCA.

5. Discussion

Proteome analysis by LC-MS/MS has been widely used for the characterization and quantification of proteins and peptides, especially in the evaluation of cancer biomarkers, including CHCA (Cevenini et al., 2020; Duangkumpha et al., 2019; Hoshino et al., 2020; Hristova and Chan, 2019; Huang et al., 2017; Janvilisri, 2015; Kim et al., 2009; Krug et al., 2020; Nunez-Naveira et al., 2019; Phanaksri et al., 2022; Prasopdee et al.,

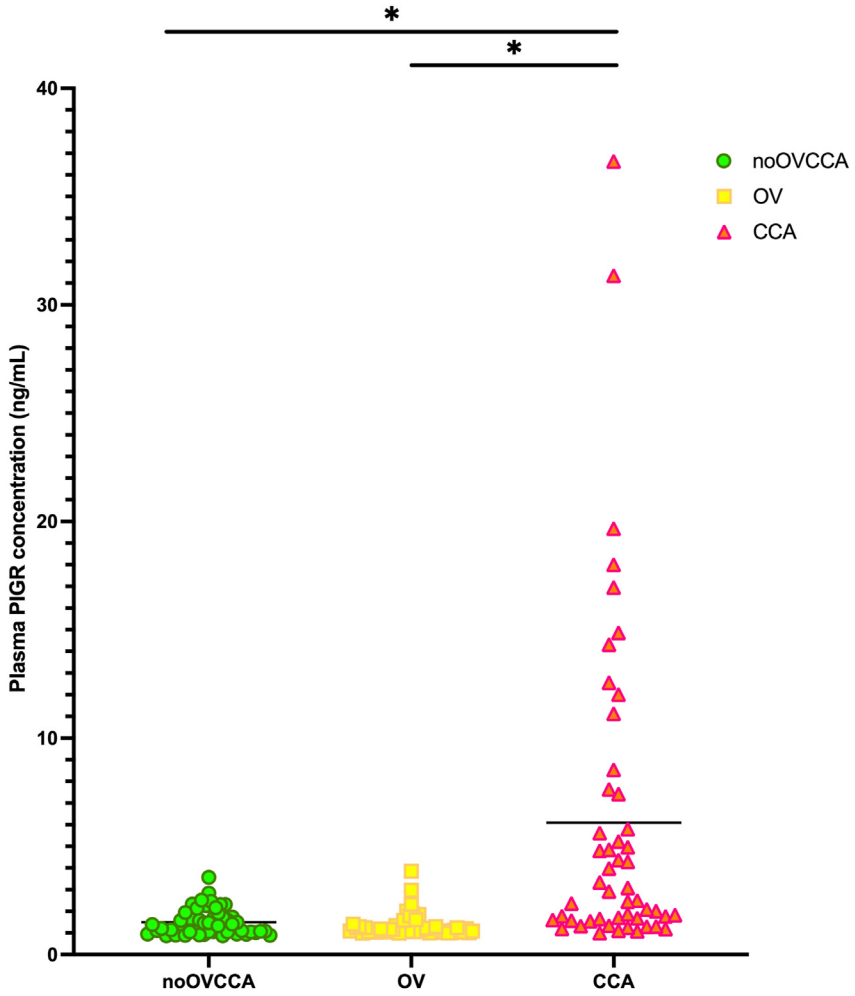

Figure 4. The plasma PIGR concentration. The circle, square, and triangle represent noOVCCA, OV, and CCA, respectively. The group is on the X-axis and the plasma PIGR concentration (ng/ml) is on the Y-axis. The PIGR level is significantly increased in the CCA group. The asterisk (*) indicates a significant difference $P < 0.01$.

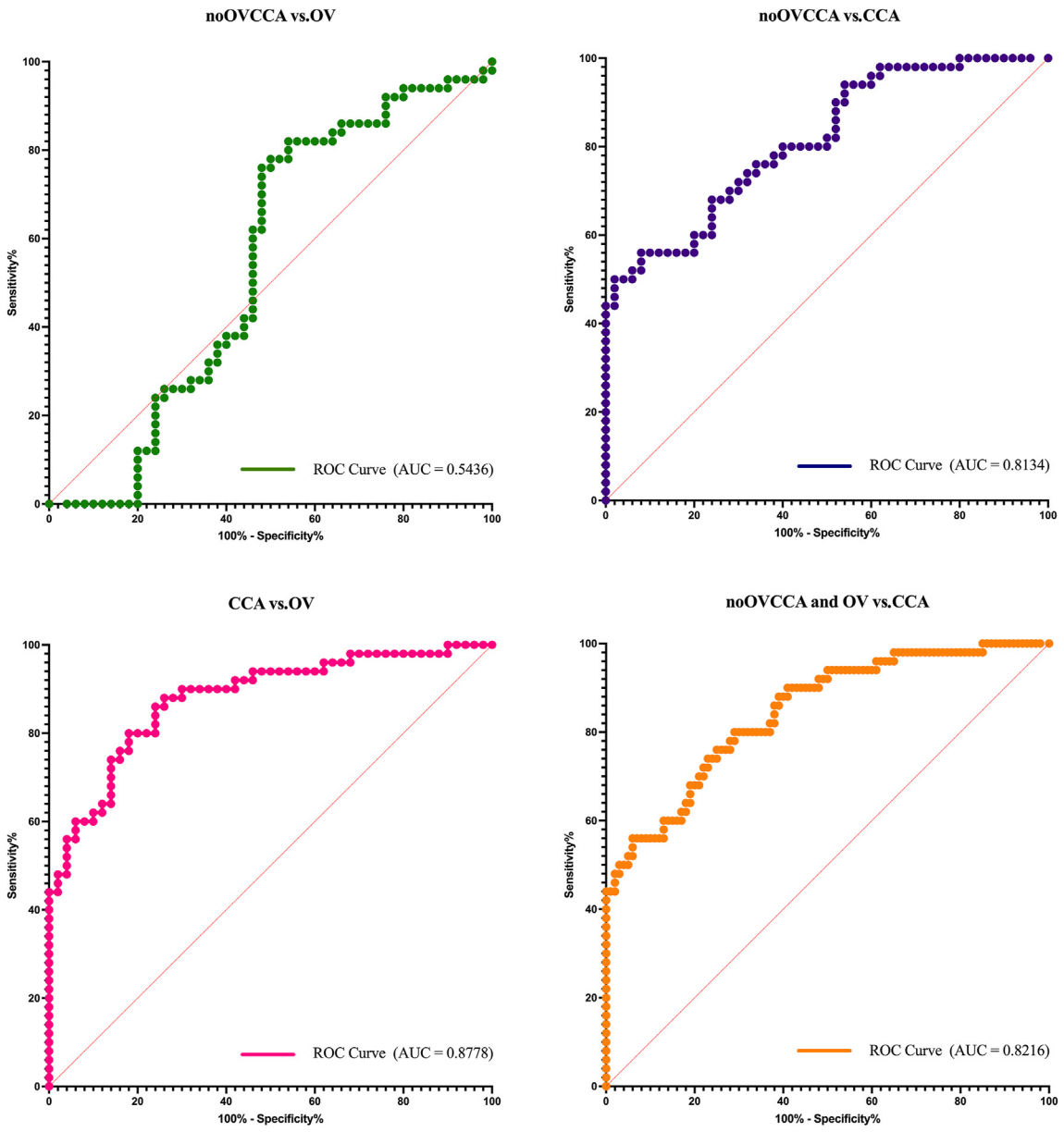

Figure 5. The AUC of the ROC curve of noOVCCA vs. OV (upper left), noOVCCA vs. CCA (upper right), CCA vs. OV (lower left), and noOVCCA and OV vs. CCA (lower right). The % sensitivity is plotted against 100% - % specificity on the X-axis and Y-axis, respectively. The AUC of ROC curves are calculated and indicated in each curve. The highest AUC was obtained in OV vs. CCA.

2022). An individual and pooled sample were used with different advantages and disadvantages. It has been estimated that thousands of individual samples are needed to reduce the biological variability and false biomarker numbers. Pooled samples can help reduce the biological variability of samples, resulting in data with a high degree of confidence (Orton and Doucette, 2013). The time and cost required to acquire individual samples were significantly higher than pooled samples. Based on the incidence of CHCA, sample variability, time, and cost, pooled plasma samples were used in this study to identify potential biomarkers for diagnostic CHCA. Two potential biomarkers for CHCA were identified—S100A9 and the polymeric immunoglobulin receptor (PIGR). S100A9 has been identified as a biomarker for several cancers (Gunaldi et al., 2015; Hermani et al., 2005; Huang et al., 2018; Kim et al., 2009; Lim et al., 2016; Liu et al., 2019; Lv et al., 2020; Meng et al., 2019; Nunez-Naveira et al., 2019; Zhou et al., 2019), including both non-*O. viverrini*-related CHCA (Shi et al., 2013) and *O. viverrini*-related CHCA (Duangkumpha et al., 2019). Meanwhile, PIGR is a biomarker for CHCA in a non-endemic area of *O. viverrini* (Arbelaiz et al., 2017). S100A9 expression was also high in PSC (Reinhard et al., 2012). Therefore, in this study, only PIGR was identified and further validated as a potential biomarker for diagnosing CHCA in the endemic area of *O. viverrini*.

Duangkumpha and colleagues identified serum S100A9 as a potential biomarker for CHCA against premalignant periductal fibrosis (PDF) and healthy subjects (Duangkumpha et al., 2019). Shi and colleagues demonstrated that S100A9 is a biomarker for CHCA by 2D-DIGE. The S100A9 immunohistochemical results demonstrated 92.6% sensitivity and 75% specificity in CHCA diagnosis (Shi et al., 2013). Puetkasichonpasutha and colleagues reported that up-regulation of S100A9 gene expression was correlated with longer survival in patients with

Table 2. Calculated diagnostic parameters of plasma PIGR concentration. The cut-off at 1.559 showed both high sensitivity and specificity and 100% specificity was obtained at the cut-off at 3.850.

	Cut-off >1.559		Cut-off >3.850	
	Value	95% CI	Value	95% CI
Sensitivity	78.00%	64.04%–88.47%	44.00%	29.99%–58.75%
Specificity	71.00%	61.07%–79.64%	100.00%	96.38%–100.00%
Positive Likelihood Ratio (PLR)	2.69	1.91–3.78	N/A	N/A
Negative Likelihood Ratio (NLR)	0.31	0.18–0.53	0.56	0.44–0.72
Positive Predictive Value (PPV)	57.35%	48.90%–65.39%	100.00%	N/A
Negative Predictive Value (NPV)	86.59%	79.05%–91.69%	78.12%	73.64%–82.03%
Accuracy	73.33%	65.51%–80.22%	81.33%	74.16%–87.22%

CHCA (Puetkasichonpasutha et al., 2020). S100A9 promotes phagocytotic action in neutrophils via the PI3K/AKT pathway, which agrees with previous reports on the up-regulation of proteins in the PI3K/AKT/MTOR pathway in CHCA (Moolthiya et al., 2014; Rizvi et al., 2014; Tiemin et al., 2020; Wu et al., 2020).

PIGR has also been previously identified as a biomarker for pancreatic cyst and pancreatic ductal adenocarcinoma (Park et al., 2015; Sogawa et al., 2016). Recently, PIGR was identified from enriched serum extracellular vesicle as a biomarker for non-*O. viverrini*-related CHCA (Arbelaiz et al., 2017), where a chronic inflammatory condition, i.e., PSC, has been identified as a premalignant lesion for CHCA. However, in non-*O. viverrini* endemic areas, PIGR western analysis using sensitivity, specificity, and AUC of 83.3%, 100%, and 0.844, respectively, could not differentiate CHCA from PSC. Thus, using PIGR in combination with other potential biomarkers has been suggested (Arbelaiz et al., 2017). In this study, patients with the *O. viverrini* infection, a risk factor for CHCA, were recruited to identify the potential of PIGR as a biomarker. The results of this study show promise of using plasma PIGR as a biomarker in detecting CHCA in simple *O. viverrini* infections and healthy subjects with substantial sensitivity, specificity, and AUC. From our results, a plasma PIGR cut-off at $>$ 1.559 ng/ml can be used for disease screening, while a plasma PIGR of $>$3.850 ng/ml strongly suggests a diagnosis of CHCA. Nevertheless, asymptomatic CHCA at an early stage, unavailable effective diagnostic methods, and only a few early stages of CHCA cases were enrolled in this study; thus, the detection of an early stage of CHCA case by PIGR may be limited. However, plasma PIGR is promising for further investigation of its efficacy in early-stage CHCA detection, especially during the transition from *O. viverrini* infection to an early-stage CHCA.

Therefore, PIGR was used in parallel with stool examination during annual health check-ups to screen for asymptomatic CHCA with a history of *O. viverrini* infection before ultrasonography of the liver. Presently, liver ultrasonography is used to screen CHCA patients, causing a burden on ultrasonography specialists. Moreover, using PIGR for prognosis is promising, as it has been related to chemoresistance and/or poor prognosis in cancers (Berntsson et al., 2014; Fristedt et al., 2014b; Liu et al., 2014; Ohkuma et al., 2020; Wang et al., 2014). This must be further investigated for efficacy in CHCA before or after surgery and chemotherapy.

Using PIGR to differentiate healthy/*O. viverrini* infection and CHCA is more suitable in endemic areas of *Ov,* such as Southeast Asian countries, while S100A9 could be used to differentiate normal/periductal fibrosis and CHCA (Duangkumpha et al., 2019). Differential diagnosis of PSC and CHCA by S100A9 was limited (Arbelaiz et al., 2017). Although the AUC of PIGR was lower than S100A9, 100% specificity can be obtained using PIGR at the cut-off at 3.850.

PIGR is a receptor for polymeric immunoglobulins such as IgA and IgM and plays a critical role in the transcytosis of IgA and IgM from the basolateral to apical surface in response to immunogens. Aberrancies in PIGR have been reported to correlate with an increase and decrease in gene expression and gene polymorphism, as found in several malignancies (Arumugam et al., 2017; Chang et al., 2005; Gologan et al., 2008; Hirunsatit et al., 2003; Ocak et al., 2012; Xiao et al., 2005). Serum levels of PIGR were high in cancer patients before surgery and decreased in the same patients post-operatively (Sogawa et al., 2016). Nevertheless, higher levels of PIGR expression were correlated with longer survival, while the low or absent expressions of PIGR were usually found in patients with lymph node metastases (Ai et al., 2011; Arumugam et al., 2017; Berntsson et al., 2014; Fristedt et al., 2014a; Gologan et al., 2008; Niu et al., 2014; Qi et al., 2016; Wang et al., 2014). Conversely, high levels of PIGR expression resulted in chemoresistance and poor prognosis in patients with pancreatic cancer (Ohkuma et al., 2020). Yue and colleagues demonstrated that PIGR promoted cell transformation and induced oncogenic growth by Yes activation in the MEK/ERK cascade (Yue et al., 2017).

In conclusion, proteomic analysis using solution-based tryptic digestion, a label-free method, Orbitrap analysis followed by high-energy collisional dissociation, and technical triplicates with five biological replicates was demonstrated to identify S100A9 and PIGR as potential biomarkers for CHCA. The plasma concentrations of PIGR showed substantial sensitivity, specificity, and accuracy as a diagnostic and screening tool for CHCA. Therefore, PIGR has great potential as a biomarker in differentiating patients with CHCA from patients with *O. viverrini* infections and healthy subjects. The application of plasma PIGR concentration holds promise in future CHCA screening and diagnostic protocols, especially in areas endemic to *O. viverrini*.

Declarations

Author contribution statement

Sattrachai Prasopdee; Yodying Yingchutrakul; Sucheewin Krobthong; Veerachai Thitapakorn, Ph.D: Conceived and designed the experiments; Performed the experiments; Analyzed and interpreted the data; Contributed reagents, materials, analysis tools or data; Wrote the paper.

Montinee Pholhelm: Performed the experiments; Analyzed and interpreted the data.

Patompon Wongtrakoongate; Kritiya Butthongkomvong: Performed the experiments; Analyzed and interpreted the data; Contributed reagents, materials, analysis tools or data.

Jutharat Kulsantiwong: Performed the experiments; Analyzed and interpreted the data.

Teva Phanaksri; Anthicha Kunjantarachot; Thanakrit Sathavornmanee: Performed the experiments; Analyzed and interpreted the data; Wrote the paper.

Smarn Tesana: Conceived and designed the experiments; Performed the experiments; Analyzed and interpreted the data; Wrote the paper.

Funding statement

Veerachai Thitapakorn was supported by Thammasat Research Unit in Opisthorchiasis, Cholangiocarcinoma, and Neglected Parasitic Diseases, Thammasat University (TRU-OCN) and Thai Government Research Fund through Thammasat University (50/2559 and 64/2560).

Sattrachai Prasopdee was supported by Thai Government Research Fund through Thammasat University (36/2562).

Data availability statement

Data associated with this study has been deposited at “Serum proteomics analysis of CCA” under the accession number “PXD028152” [10.6019/PXD028152].

Declaration of interest's statement

The authors declare no conflict of interest.

Additional information

Supplementary content related to this article has been published online at https://doi.org/10.1016/j.heliyon.2022.e10965.

Acknowledgements

The authors acknowledge the Central Instrument Facility, Faculty of Science, Mahidol University for supporting Thermo Scientific™ Q Exactive™ HF hybrid quadrupole-Orbitrap mass spectrometer and UltiMate 300 LC system. Veerachai Thitapakorn was supported by Thammasat Research Unit in Opisthorchiasis, Cholangiocarcinoma, and Neglected Parasitic Diseases, Thammasat University (TRU-OCN) and Thai Government Research Fund through Thammasat University (50/2559 and 64/2560). Sattrachai Prasopdee was supported by Thai Government Research Fund through Thammasat University (36/2562).

References

Ai, J., Tang, Q., Wu, Y., Xu, Y., Feng, T., Zhou, R., Chen, Y., Gao, X., Zhu, Q., Yue, X., et al., 2011. The role of polymeric immunoglobulin receptor in inflammation-induced tumor metastasis of human hepatocellular carcinoma. J. Natl. Cancer Inst. 103, 1696–1712.

Arbelaiz, A., Azkargorta, M., Krawczyk, M., Santos-Laso, A., Lapitz, A., Perugorria, M.J., Erice, O., Gonzalez, E., Jimenez-Aguero, R., Lacasta, A., et al., 2017. Serum extracellular vesicles contain protein biomarkers for primary sclerosing cholangitis and cholangiocarcinoma. Hepatology 66, 1125–1143.

Arumugam, P., Bhattacharya, S., Chin-Aleong, J., Capasso, M., Kocher, H.M., 2017. Expression of polymeric immunoglobulin receptor and stromal activity in pancreatic ductal adenocarcinoma. Pancreatology 17, 295–302.

Banales, J.M., Marin, J.J.G., Lamarca, A., Rodrigues, P.M., Khan, S.A., Roberts, L.R., Cardinale, V., Carpino, G., Andersen, J.B., Braconi, C., et al., 2020. Cholangiocarcinoma 2020: the next horizon in mechanisms and management. Nat. Rev. Gastroenterol. Hepatol. 17, 557–588.

Bardou, P., Mariette, J., Escudié, F., Djemiel, C., Klopp, C., 2014. jvenn: an interactive Venn diagram viewer. BMC Bioinf. 15, 293.

Berntsson, J., Lundgren, S., Nodin, B., Uhlen, M., Gaber, A., Jirstrom, K., 2014. Expression and prognostic significance of the polymeric immunoglobulin receptor in epithelial ovarian cancer. J. Ovarian Res. 7, 26.

Boondit, J., Suwannahitatorn, P., Siripattanapipong, S., Leelayoova, S., Mungthin, M., Tan-Ariya, P., Piyaraj, P., Naaglor, T., Ruang-Areerate, T., 2020. An epidemiological survey of *Opisthorchis viverrini* infection in a lightly infected community, eastern Thailand. Am. J. Trop. Med. Hyg. 102, 838–843.

Cevenini, A., Orru, S., Imperlini, E., 2020. Secretome proteomic approaches for biomarker discovery: an update on colorectal cancer. Medicina (Kaunas) 56.

Chang, Y., Lee, T.C., Li, J.C., Lai, T.L., Chua, H.H., Chen, C.L., Doong, S.L., Chou, C.K., Sheen, T.S., Tsai, C.H., 2005. Differential expression of osteoblast-specific factor 2 and polymeric immunoglobulin receptor genes in nasopharyngeal carcinoma. Head Neck 27, 873–882.

Duangkumpha, K., Stoll, T., Phetcharaburanin, J., Yongvanit, P., Thanan, R., Techasen, A., Namwat, N., Khuntikeo, N., Chamadol, N., Roytrakul, S., et al., 2019. Discovery and qualification of serum protein biomarker candidates for cholangiocarcinoma diagnosis. J. Proteome Res. 18, 3305–3316.

Fristedt, R., Elebro, J., Gaber, A., Jonsson, L., Heby, M., Yudina, Y., Nodin, B., Uhlen, M., Eberhard, J., Jirstrom, K., 2014a. Reduced expression of the polymeric immunoglobulin receptor in pancreatic and periampullary adenocarcinoma signifies tumour progression and poor prognosis. PLoS One 9, e112728.

Fristedt, R., Gaber, A., Hedner, C., Nodin, B., Uhlen, M., Eberhard, J., Jirstrom, K., 2014b. Expression and prognostic significance of the polymeric immunoglobulin receptor in esophageal and gastric adenocarcinoma. J. Transl. Med. 12, 83.

Gologan, A., Acquafondata, M., Dhir, R., Sepulveda, A.R., 2008. Polymeric immunoglobulin receptor-negative tumors represent a more aggressive type of adenocarcinomas of distal esophagus and gastroesophageal junction. Arch. Pathol. Lab Med. 132, 1295–1301.

Gunaldi, M., Okuturlar, Y., Gedikbasi, A., Akarsu, C., Karabulut, M., Kural, A., 2015. Diagnostic importance of S100A9 and S100A12 in breast cancer. Biomed. Pharmacother. 76, 52–56.

Haw, R., Hermjakob, H., D'Eustachio, P., Stein, L., 2011. Reactome pathway analysis to enrich biological discovery in proteomics data sets. Proteomics 11, 3598–3613.

Hermani, A., Hess, J., De Servi, B., Medunjanin, S., Grobholz, R., Trojan, L., Angel, P., Mayer, D., 2005. Calcium-binding proteins S100A8 and S100A9 as novel diagnostic markers in human prostate cancer. Clin. Cancer Res. 11, 5146–5152.

Hirunsatit, R., Kongruttanachok, N., Shotelersuk, K., Supiyaphun, P., Voravud, N., Sakuntabhai, A., Mutirangura, A., 2003. Polymeric immunoglobulin receptor polymorphisms and risk of nasopharyngeal cancer. BMC Genet. 4, 3.

Hoshino, A., Kim, H.S., Bojmar, L., Gyan, K.E., Cioffi, M., Hernandez, J., Zambirinis, C.P., Rodrigues, G., Molina, H., Heissel, S., et al., 2020. Extracellular vesicle and particle biomarkers define multiple human cancers. Cell 182, 1044–1061 e1018.

Hristova, V.A., Chan, D.W., 2019. Cancer biomarker discovery and translation: proteomics and beyond. Expert Rev. Proteomics 16, 93–103.

Huang, H., Huang, Q., Tang, T., Gu, L., Du, J., Li, Z., Lu, X., Zhou, X., 2018. Clinical significance of calcium-binding protein S100A8 and S100A9 expression in non-small cell lung cancer. Thorac Cancer 9, 800–804.

Huang, Z., Ma, L., Huang, C., Li, Q., Nice, E.C., 2017. Proteomic profiling of human plasma for cancer biomarker discovery. Proteomics 17.

IARC, 1994. Infection with liver flukes (*Opisthorchis viverrini, Opisthorchis felineus* and *Clonorchis sinensis*). IARC Monogr. Eval. Carcinog. Risks Hum. 61, 121–175.

Janvilisri, T., 2015. Omics-based identification of biomarkers for nasopharyngeal carcinoma. Dis. Markers 2015, 762128.

Kim, H.J., Kang, H.J., Lee, H., Lee, S.T., Yu, M.H., Kim, H., Lee, C., 2009. Identification of S100A8 and S100A9 as serological markers for colorectal cancer. J. Proteome Res. 8, 1368–1379.

Krobthong, S., Choowongkomon, K., Suphakun, P., Kuaprasert, B., Samutrtai, P., Yingchutrakul, Y., 2021. The anti-oxidative effect of Lingzhi protein hydrolysates on lipopolysaccharide-stimulated A549 cells. Food Biosci. 41, 101093.

Krobthong, S., Yingchutrakul, Y., Samutrtai, P., Hitakarun, A., Siripattanapipong, S., Leelayoova, S., Mungthin, M., Choowongkomon, K., 2022. Utilizing quantitative proteomics to identify species-specific protein therapeutic targets for the treatment of Leishmaniasis. ACS Omega 7, 12580–12588.

Krug, K., Jaehnig, E.J., Satpathy, S., Blumenberg, L., Karpova, A., Anurag, M., Miles, G., Mertins, P., Geffen, Y., Tang, L.C., et al., 2020. Proteogenomic Landscape of breast cancer tumorigenesis and targeted therapy. Cell 183, 1436 e1431–1456 e1431.

Lim, S.Y., Yuzhalin, A.E., Gordon-Weeks, A.N., Muschel, R.J., 2016. Tumor-infiltrating monocytes/macrophages promote tumor invasion and migration by upregulating S100A8 and S100A9 expression in cancer cells. Oncogene 35, 5735–5745.

Liu, F., Ye, P., Bi, T., Teng, L., Xiang, C., Wang, H., Li, Y., Jin, K., Mou, X., 2014. COLORECTAL polymeric immunoglobulin receptor expression is correlated with hepatic metastasis and poor prognosis in colon carcinoma patients with hepatic metastasis. Hepato-Gastroenterology 61, 652–659.

Liu, Y., Luo, G., He, D., 2019. Clinical importance of S100A9 in osteosarcoma development and as a diagnostic marker and therapeutic target. Bioengineered 10, 133–141.

Lv, Z., Li, W., Wei, X., 2020. S100A9 promotes prostate cancer cell invasion by activating TLR4/NF-kappaB/integrin beta1/FAK signaling. OncoTargets Ther. 13, 6443–6452.

Maleewong, W., Intapan, P., Wongwajana, S., Sitthithaworn, P., Pipitgool, V., Wongkham, C., Daenseegaew, W., 1992. Prevalence and intensity of *Opisthorchis viverrini* in rural community near the Mekong River on the Thai-Laos border in northeast Thailand. J. Med. Assoc. Thai. 75, 231–235.

Meng, J., Gu, F., Fang, H., Qu, B., 2019. Elevated serum S100A9 indicated poor prognosis in hepatocellular carcinoma after curative resection. J. Cancer 10, 408–415.

Moolthiya, P., Tohtong, R., Keeratichamroen, S., Leelawat, K., 2014. Role of mTOR inhibitor in cholangiocarcinoma cell progression. Oncol. Lett. 7, 854–860.

Niu, H., Wang, K., Wang, Y., 2014. Polymeric immunoglobulin receptor expression is predictive of poor prognosis in glioma patients. Int. J. Clin. Exp. Med. 7, 2185–2190.

Nunez-Naveira, L., Marinas-Pardo, L.A., Montero-Martinez, C., 2019. Mass spectrometry analysis of the exhaled breath condensate and proposal of dermcidin and S100A9 as possible markers for lung cancer prognosis. Lung 197, 523–531.

Ocak, S., Pedchenko, T.V., Chen, H., Harris, F.T., Qian, J., Polosukhin, V., Pilette, C., Sibille, Y., Gonzalez, A.L., Massion, P.P., 2012. Loss of polymeric immunoglobulin receptor expression is associated with lung tumourigenesis. Eur. Respir. J. 39, 1171–1180.

Ohkuma, R., Yada, E., Ishikawa, S., Komura, D., Kubota, Y., Hamada, K., Horiike, A., Ishiguro, T., Hirasawa, Y., Ariizumi, H., et al., 2020. High expression levels of polymeric immunoglobulin receptor are correlated with chemoresistance and poor prognosis in pancreatic cancer. Oncol. Rep. 44, 252–262.

Orton, D.J., Doucette, A.A., 2013. Proteomic workflows for biomarker identification using mass spectrometry - technical and statistical considerations during initial discovery. Proteomes 1, 109–127.

Park, S.J., Gu, M.J., Lee, D.S., Yun, S.S., Kim, H.J., Choi, J.H., 2015. EGFR expression in pancreatic intraepithelial neoplasia and ductal adenocarcinoma. Int. J. Clin. Exp. Pathol. 8, 8298–8304.

Phanaksri, T., Yingchutrakul, Y., Roytrakul, S., Prasopdee, S., Kunjantarachot, A., Butthongkomvong, K., Tesana, S., Sathavornmanee, T., Thitapakorn, V., 2022. Plasma checkpoint protein 1 (Chk1) as a potential diagnostic biomarker for opisthorchiasis and cholangiocarcinoma. Cancer Biomark 33, 43–55.

Pinlaor, S., Yongvanit, P., Hiraku, Y., Ma, N., Semba, R., Oikawa, S., Murata, M., Sripa, B., Sithithaworn, P., Kawanishi, S., 2003. 8-nitroguanine formation in the liver of hamsters infected with *Opisthorchis viverrini*. Biochem. Biophys. Res. Commun. 309, 567–571.

Pinlaor, S., Yongvanit, P., Prakobwong, S., Kaewsamut, B., Khoontawad, J., Pinlaor, P., Hiraku, Y., 2009. Curcumin reduces oxidative and nitrative DNA damage through balancing of oxidant-antioxidant status in hamsters infected with *Opisthorchis viverrini*. Mol. Nutr. Food Res. 53, 1316–1328.

Prakobwong, S., Khoontawad, J., Yongvanit, P., Pairojkul, C., Hiraku, Y., Sithithaworn, P., Pinlaor, P., Aggarwal, B.B., Pinlaor, S., 2011. Curcumin decreases cholangiocarcinogenesis in hamsters by suppressing inflammation-mediated molecular events related to multistep carcinogenesis. Int. J. Cancer 129, 88–100.

Prasopdee, S., Yingchutrakul, Y., Roytrakul, S., Pholhelm, M., Phanaksri, T., Kunjantarachot, A., Kulsantiwong, J., Butthongkomvong, K., Tesana, S., Sathavornmanee, T., Thitapakorn, V., 2022. Phosphatidylinositol 4,5-bisphosphate 3-kinase catalytic subunit beta as a potential biomarker for *Opisthorchis viverrini* infection and cholangiocarcinoma. Parasitology 149, 171–180.

Puetkasichonpasutha, J., Namwat, N., Sa-Ngiamwibool, P., Titapun, A., Suthiphongchai, T., 2020. Evaluation of p53 and its target gene expression as potential biomarkers of cholangiocarcinoma in Thai patients. Asian Pac. J. Cancer Prev. APJCP 21, 791–798.

Qi, X., Li, X., Sun, X., 2016. Reduced expression of polymeric immunoglobulin receptor (pIgR) in nasopharyngeal carcinoma and its correlation with prognosis. Tumour Biol. 37, 11099–11104.

Reinhard, L., Rupp, C., Riedel, H.D., Ruppert, T., Giese, T., Flechtenmacher, C., Weiss, K.H., Kloeters-Plachky, P., Stremmel, W., Schirmacher, P., et al., 2012. S100A9 is a biliary protein marker of disease activity in primary sclerosing cholangitis. PLoS One 7, e29821.

Rizvi, S., Borad, M.J., Patel, T., Gores, G.J., 2014. Cholangiocarcinoma: molecular pathways and therapeutic opportunities. Semin. Liver Dis. 34, 456–464.

Shi, Y., Deng, X., Zhan, Q., Shen, B., Jin, X., Zhu, Z., Chen, H., Li, H., Peng, C., 2013. A prospective proteomic-based study for identifying potential biomarkers for the diagnosis of cholangiocarcinoma. J. Gastrointest. Surg. 17, 1584–1591.

Sogawa, K., Takano, S., Iida, F., Satoh, M., Tsuchida, S., Kawashima, Y., Yoshitomi, H., Sanda, A., Kodera, Y., Takizawa, H., et al., 2016. Identification of a novel serum biomarker for pancreatic cancer, C4b-binding protein alpha-chain (C4BPA) by quantitative proteomic analysis using tandem mass tags. Br. J. Cancer 115, 949–956.

Steele, J.A., Richter, C.H., Echaubard, P., Saenna, P., Stout, V., Sithithaworn, P., Wilcox, B.A., 2018. Thinking beyond *Opisthorchis viverrini* for risk of cholangiocarcinoma in the lower Mekong region: a systematic review and meta-analysis. Infect. Dis. Poverty 7, 44.

Szklarczyk, D., Gable, A.L., Nastou, K.C., Lyon, D., Kirsch, R., Pyysalo, S., Doncheva, N.T., Legeay, M., Fang, T., Bork, P., et al., 2021. The STRING database in 2021: customizable protein-protein networks, and functional characterization of user-uploaded gene/measurement sets. Nucleic Acids Res. 49, D605–d612.

Tiemin, P., Fanzheng, M., Peng, X., Jihua, H., Ruipeng, S., Yaliang, L., Yan, W., Junlin, X., Qingfu, L., Zhefeng, H., et al., 2020. MUC13 promotes intrahepatic cholangiocarcinoma progression via EGFR/PI3K/AKT pathways. J. Hepatol. 72, 761–773.

Vizcaino, J.A., Cote, R.G., Csordas, A., Dianes, J.A., Fabregat, A., Foster, J.M., Griss, J., Alpi, E., Birim, M., Contell, J., et al., 2013. The PRoteomics IDEntifications (PRIDE) database and associated tools: status in 2013. Nucleic Acids Res. 41, D1063–1069.

Wang, X., Du, J., Gu, P., Jin, R., Lin, X., 2014. Polymeric immunoglobulin receptor expression is correlated with poor prognosis in patients with osteosarcoma. Mol. Med. Rep. 9, 2105–2110.

Wu, Q., Fan, H., Lang, R., Li, X., Zhang, X., Lv, S., He, Q., 2020. Overexpression of 14-3-3sigma modulates cholangiocarcinoma cell survival by PI3K/akt signaling. BioMed Res. Int. 2020, 3740418.

Xiao, T., Ying, W., Li, L., Hu, Z., Ma, Y., Jiao, L., Ma, J., Cai, Y., Lin, D., Guo, S., et al., 2005. An approach to studying lung cancer-related proteins in human blood. Mol. Cell. Proteomics 4, 1480–1486.

Yue, X., Ai, J., Xu, Y., Chen, Y., Huang, M., Yang, X., Hu, B., Zhang, H., He, C., Yang, X., et al., 2017. Polymeric immunoglobulin receptor promotes tumor growth in hepatocellular carcinoma. Hepatology 65, 1948–1962.

Zhou, M., Li, M., Liang, X., Zhang, Y., Huang, H., Feng, Y., Wang, G., Liu, T., Chen, Z., Pei, H., Chen, Y., 2019. The significance of serum S100A9 and TNC levels as biomarkers in colorectal cancer. J. Cancer 10, 5315–5323.